

MOST satellite photometry of stars in the M67 field: Eclipsing binaries, blue stragglers and δ Scuti variables*

Theodor Pribulla^{1,2}, Slavek Rucinski¹, Jaymie M. Matthews³, Rainer Kuschnig⁴,
Jason F. Rowe³, David B. Guenther⁵, Anthony F. J. Moffat⁶, Dimitar Sasselov⁷,
Gordon A. H. Walker³, Werner W. Weiss⁴

¹*Department of Astronomy and Astrophysics, University of Toronto, 50 St. George Street, Toronto, ON, M5S 3H4, Canada,
E-mail: pribulla@ta3.sk, rucinski@astro.utoronto.ca*

²*Astronomical Institute, Slovak Academy of Sciences, 059 60 Tatranská Lomnica, Slovakia*

³*Department of Physics & Astronomy, University of British Columbia, 6224 Agricultural Road,
Vancouver, B.C., V6T 1Z1, Canada*

⁴*Institut für Astronomie, Universität Wien, Türkenschanzstrasse 17, A-1180 Wien, Austria*

⁵*Institute for Computational Astrophysics, Department of Astronomy and Physics, Saint Mary's University,
Halifax, NS, B3H 3C3, Canada*

⁶*Observatoire Astronomique du Mont Mégantic, Département de Physique, Université de Montréal, C.P.6128,
Succursale: Centre-Ville, Montréal, QC, H3C 3J7, Canada*

⁷*Harvard-Smithsonian Center for Astrophysics, 60 Garden Street, Cambridge, MA 02138, USA*

Accepted 0000 Month 00. Received 0000 Month 00; in original form 2007 March 17

ABSTRACT

We present two series of MOST (Microvariability & Oscillations of STars) space-based photometry, covering nearly continuously 10 days in 2004 and 30 days in 2007, of selected variable stars in the upper Main Sequence of the old open cluster M67. New high-precision light curves were obtained for the blue-straggler binary/triple systems AH Cnc, ES Cnc and EV Cnc. The precision and phase coverage of ES Cnc and EV Cnc is by far superior to any previous observations. The light curve of ES Cnc is modelled in detail, assuming two dark photospheric spots and Roche geometry. An analysis of the light curve of AH Cnc indicates a low mass ratio ($q \sim 0.13$) and a high inclination angle for this system. Two new long-period eclipsing binaries, GSC 814–323 and HD 75638 (non-members of M67) were discovered. We also present ground-based DDO spectroscopy of ES Cnc and of the newly found eclipsing binaries. Especially interesting is HD 75638, a member of a visual binary, which must itself be a triple or a higher-multiplicity system. New light curves of two δ Scuti pulsators, EX Cnc and EW Cnc, have been analyzed leading to detection of 26 and 8 pulsation frequencies of high temporal stability.

Key words: stars: close binaries - stars: eclipsing binaries – stars: variable stars

1 INTRODUCTION

M67 (NGC 2682) is one of the best studied open clusters. It is also one of the oldest known galactic clusters, with an estimated age of about 4 Gyr. Other parameters of the cluster are: $E(B-V) = 0.05$ and distance modulus $(m-M_V) = 9.59$

(Montgomery et al. 1993). M67 contains a high percentage of blue stragglers, stars which are bluer and more luminous than the main sequence turnoff point of the cluster. For M67, the turnoff occurs near $B - V = 0.55$, and $V = 13.0$. The formation mechanism of blue stragglers is still debated, but the most probable scenario is via mass transfer or mergers in close binaries (Bailyn 1995). Several blue stragglers in M67 are known to be eclipsing binaries, which supports this hypothesis. The large number of close binaries in M67 is suggested by the relatively large number (25) of X-ray sources (Belloni et al. 1998). In such an old cluster, the X-ray sources cannot be single rapidly-rotating stars, but – more likely – are tidally locked components of close bina-

* Based on photometric data from MOST, a Canadian Space Agency mission (jointly operated by Dynacon Inc., the University of Toronto Institute for Aerospace Studies and the University of British Columbia, with the assistance of the University of Vienna), and on spectroscopic data from the David Dunlap Observatory, University of Toronto

ries. In addition, long-term spectroscopic surveys of M67 (Milone & Latham 1992; Latham & Milone 1996) revealed among the blue stragglers, 5 spectroscopic binaries with orbital periods between 850 – 5000 days.

In this paper, we present two time series of rapid, quasi-continuous photometry for selected targets in M67 obtained with the MOST (Microvariability & Oscillations of STars) satellite in 2004 and 2007. The targets were selected primarily to study two domains of cluster objects accessible to a small telescope like MOST: the upper Main Sequence (mostly blue stragglers) and red giants. Here we describe the results for the former group of objects, including two δ Scuti, while a future paper (Kallinger et al., in preparation) will describe analyses and asteroseismology of the p-mode pulsations of the red giants in the cluster.

The main goals of the observations in the context of this paper were twofold: (i) a search for new variables with very small amplitudes, and (ii) obtaining high-quality light curves, particularly for blue stragglers with periods close to one day which are difficult to sample properly with ground-based observations. As we describe in Section 2, the 2004 observations were experimental and short (compared to other MOST runs), while the scope of the 2007 observations was much expanded to include time series photometry of a large number of guide stars in the M67 field. The photometric observations of MOST have been augmented by medium-dispersion spectroscopy performed at the David Dunlap Observatory (DDO).

The paper is organized as follows: Section 2 presents MOST time-series photometry and spectroscopic observations performed at the DDO. The light variations are described in Section 3 while a detailed discussion of individual binary systems known or found to be variable is given in Section 4. The δ Scuti pulsating stars are discussed separately in Section 5. The paper is concluded with the summary of the results in Section 6.

2 OBSERVATIONS

2.1 MOST photometry

MOST (Microvariability & Oscillations of STars) is a microsatellite housing a 15-cm telescope which feeds a CCD photometer through a single, custom, broadband optical filter (350 - 700 nm). The pre-launch characteristics of the mission are described by Walker et al. (2003) and the initial post-launch performance by Matthews et al. (2004). MOST is in a Sun-synchronous polar orbit (820 km altitude) from which it can monitor some stars for as long as 2 months without interruption. The instrument was designed to obtain highly precise photometry of single, bright stars through Fabry lens imaging. Since the launch, the satellite capabilities have been expanded to obtain Direct Imaging photometry of fainter stars in sub-rasters of the open area of the Science CCD, and to obtain photometry of the guide stars used to orient the spacecraft. Both observing modes yield the same time sampling and coverage as the Primary Science Target in the MOST field.

MOST was never originally intended to obtain photometry of stars fainter than $V \sim 6$, nor of multiple targets in a stellar cluster field. Its pre-launch mission goals were aster-

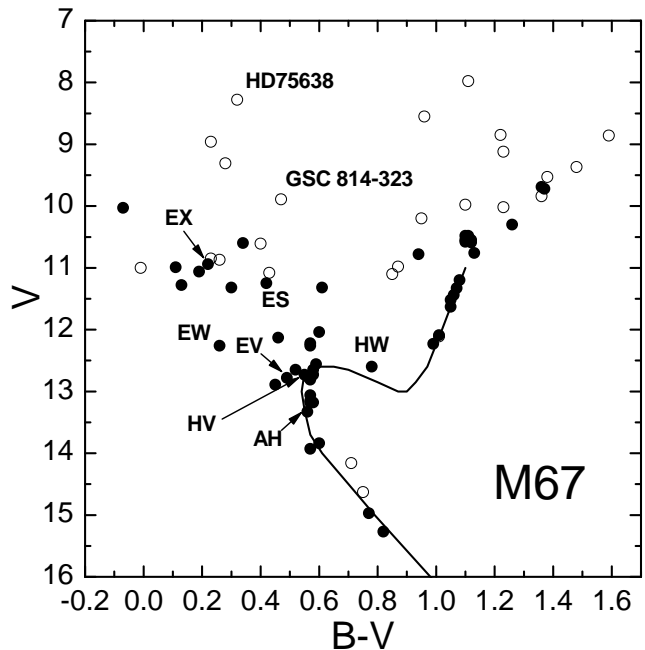


Figure 1. The colour – magnitude diagram of M67 indicating all targets observed by MOST in the field. The M67 members are marked by filled circles while non-members are marked by open circles. The variables reported in this paper are labelled by their variable star names. The $(B - V)$ colours and V magnitudes are from Montgomery et al. (1993); for non-members, we adopted the data from the TYCHO2 catalogue (Høg et al. 2000). The solid curve represents the fiducial isochrone for M67.

oseismology of bright solar-type stars, Wolf-Rayet and magnetic pulsating stars. The lack of multicolour measurements with MOST limits detailed modelling of the light curves of eclipsing binaries, particularly with components of very different spectral types. However, the ability to monitor such systems nearly continuously for weeks at a time leads to excellent light curves which are useful for variable star detection and for studies of variables whose periods are close to an integer number of days.

With 3 arcsec pixels and the $1k \times 1k$ CCD detector, the field of view of the open area of the MOST Science CCD is about $0.75^\circ \times 0.5^\circ$ (part of the field is taken by the Fabry lenses). This is larger than the size of the inner part of the M67 cluster as defined by its brightest stars. As a result, we could include as guide stars and obtain photometry for several stars which are close to M67, but are not members of the cluster. Two of these stars (HD 75638 and GSC 814-323) were found to be eclipsing binaries (or multiple systems containing an eclipsing binary).

The first series of M67 observations was 10 days long, during 13 - 23 February 2004 and was designed as a test of MOST extended capability. In this run, 30 objects were observed in the direct imaging mode in small sub-rasters of various sizes. The second run covered 30 days during 12 February - 14 March 2007. The pointing performance of the spacecraft had been dramatically improved by this time, and the guide star photometric capability had been implemented. In this run, about 40 guide stars were monitored with an additional 6 stars observed as direct imaging targets. About 3/4 through this second observing run (on

5 March 2007), the roll angle of the satellite was changed to reduce the amount of scattered Earthshine on the MOST focal plane. As a result of the change in focal plane orientation, 38 of the original 42 guide stars could be retained, and 6 new ones were added for the remainder of the run. There was no change in the selection of direct imaging targets after the roll change. All the MOST M67 targets are marked in the colour – magnitude diagram of M67 in Fig. 1.

MOST Guide Star photometry was processed on board the satellite. Direct imaging data were processed on the ground, after downloading of the six 20×20 -pixel sub-rasters (for the 2007 run) centred on target stars, much like conventional CCD photometry. In January 2006, MOST lost use of its startracker CCD due to a severe charged particle strike, and since then, both satellite attitude control and science functions have been shared by the Science CCD. This means that individual exposures must be now relatively short (less than 3.5 sec) to update the pointing information sufficiently rapidly. Hence, we stack exposures on board to achieve high S/N values. During the 2007 run, stacks consisted typically of 14 exposures, each 1.5 sec long. For the faintest stars, the cumulative CCD readout noise for the stacked exposures is the dominant noise source.

A list of the observed stars is given in Table 1. All the raw data and the reduced light curves presented in this paper are available in the MOST Public Data Archive, accessed through the Science Page of the MOST Mission web site at www.astro.ubc.ca/MOST.

In 2007, six known blue stragglers (Sanders 1036, 1082, 1263, 1280, 1282, 1284) were observed in the direct imaging mode. S1082 (ES Cnc) was monitored as a guide star and in the direct imaging mode. The latter mode, being similar to conventional CCD area photometry, produces the more precise photometry. An attempt was made to analyse photometry of five guide stars (HD 75784, BD +13°2006, HD 75717, SAO 98164 and GSC 816-2629) used for the 2004 run, but the short exposures (and lack of onboard stacking) and the larger pointing wander experienced earlier in the MOST mission, meant a relatively large photometric scatter for those targets. The focal plane scale of 3 arcsec per pixel, the pointing wander of a few pixels in the 2004 data and the typical FWHM of 2.5 pixels led to blending of images which was a serious concern for visual pairs separated by less than 10–15 arcsec.

2.2 DDO spectroscopy

After the two MOST photometric runs, spectroscopic observations of selected M67 targets were obtained using the slit spectrograph at the Cassegrain focus of the 1.88-m telescope of the David Dunlap Observatory. The spectra were taken in a wavelength window about 240 \AA wide around the MgI triplet (5167, 5173 and 5184 \AA) with an effective resolving power of $R = 12,000 - 14,000$. The diffraction grating with 2160 lines/mm was used giving the scale of $0.117 \text{ \AA}/\text{pixel}$. One-dimensional spectra were extracted by the usual procedures within the IRAF environment¹ after bias subtraction and flat field division. Cosmic ray trails were removed using

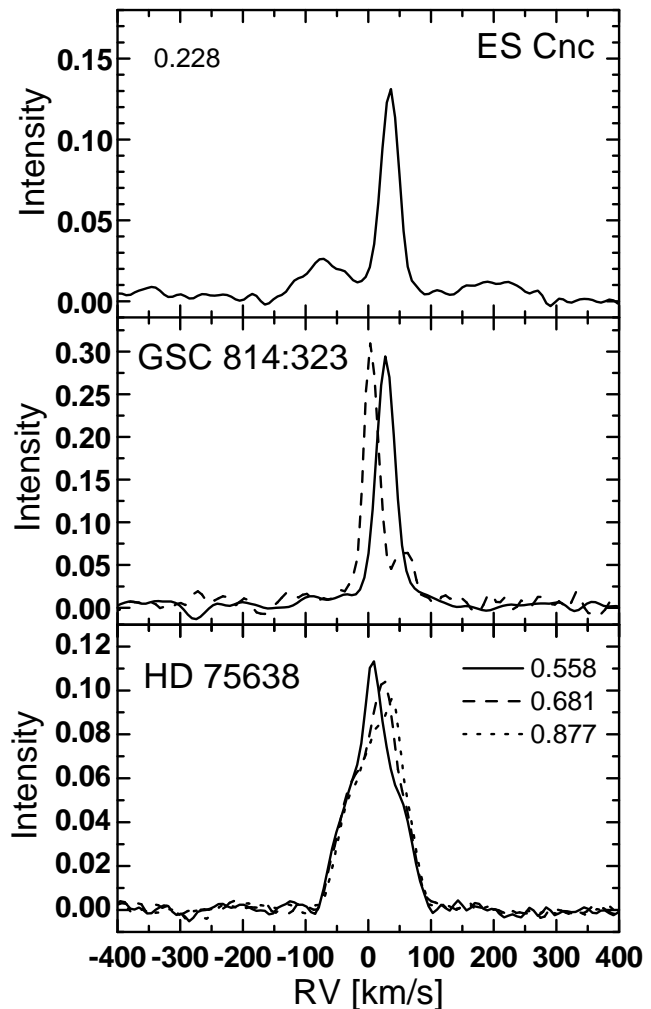


Figure 2. Broadening functions (BFs) of eclipsing variables ES Cnc, GSC 814-323 and HD 75638. For HD 75638, we show the BFs for a few orbital phases calculated from the known ephemerides as in Table 2. ES Cnc exhibits very well defined signatures of two rapidly rotating components and of a third, slowly rotating component. This system deserves to be the subject of further study using the BF approach.

the program of Pych (2004). The observations were analysed with the technique of broadening functions (BFs), described by Rucinski (1992) and Rucinski (2002), using spectra of slowly rotating stars of similar spectral type as templates. A sample of extracted BFs is given in Fig. 2.

The DDO observations are part of a more extensive spectroscopic survey (Pribulla et al., 2008, in preparation) of variable stars detected or observed during the MOST mission, especially those for which no reliable spectral classifications exist in the literature. The goals of this survey are to: (i) determine the spectral type and luminosity class, (ii) help identify the type of variability in conjunction with the MOST photometry, (iii) measure the projected rotational velocity $v \sin i$, and to (iv) detect and study the spectroscopic binaries and multiple systems in the sample (for

¹ IRAF is distributed by the National Optical Astronomy Observatories, which are operated by the Association of Universities for

Research in Astronomy, Inc., under cooperative agreement with the NSF.

Table 1. List of stars in M67 observed by the MOST satellite

GSC	α	δ	V	$B - V$	Sand.	MMJ	Other	M67	Obs	Sp. type	Type
813-1617	08 49 34.65	11 51 25.7	9.53	1.38	258	6469	BD+12 1913	N	-GG	K2	
813-2033	08 49 43.46	11 48 38.9	11.00	-0.01	376			N	-GG		
813-2806	08 49 50.15	11 25 33.7	10.20	0.95	335		BD+11 1920	N	--G		
813-1719	08 49 55.22	11 15 10.8	8.55	0.96			SAO98150	?	--G	G5	
813-2344	08 49 56.83	11 41 33.1	9.84	1.36	364	6470	BD+12 1917	N	--G		
813-2339	08 50 00.59	11 43 58.0	10.98	0.87	477			N	-GG		
813-1152	08 50 02.40	11 55 24.8	9.12	1.23	495		BD+12 1918	?	-GG	K0	
813-1032	08 50 12.30	11 51 24.5	8.86	1.59	488	6471	BD+12 1919	N	-GG	K5	
813-1419	08 50 18.29	11 55 21.4	9.98	1.10	494	6472	BD+12 1920	N	--G		
813-2055	08 50 18.62	11 24 28.4	8.85	1.22	440		SAO98156	N	--G	K0	
813-2651	08 50 19.91	11 21 30.6	9.31	0.28	436		SAO98157	N	--G	A5	
816-2629	08 50 23.71	12 56 14.8	10.61	0.40				N	G--		
816-1780	08 50 50.83	12 59 05.2	10.85	0.23			BD+13 1999	N	G--	K5	
813-1353	08 50 55.70	11 52 14.7	12.04	0.60	792	6477		Y	DGG	F5III	BS
813-2069	08 50 56.15	11 51 55.7	14.63	0.75	790	5302		N	D--	G7V	
813-2019	08 51 02.03	11 45 18.6	14.97	0.77	754	5372		Y	D--	G7V	
813-2294	08 51 03.47	11 45 01.8	11.32	0.30	752	6476		Y	DGG	A7.2:m	BS
814-1795	08 51 11.76	11 45 22.0	10.03	-0.07	977	6481		Y	-GG	B8V	BS
814-1099	08 51 12.68	11 52 42.2	10.59	1.12	1074	6492		Y	-GG	G8III	RG
814-1931	08 51 14.32	11 45 00.0	11.08	0.43	975	6480		N	-GG	F3	
814-1491	08 51 14.78	11 47 24.2	12.81	0.57	1003	5562		Y	D--	F8V	
814-1647	08 51 15.46	11 47 31.6	12.65	0.52	1005	5571		Y	D--	F2	BS
814-1735	08 51 16.84	11 45 41.8	14.16	0.71	981	5594		N	D--	G6V	
814-1763	08 51 16.98	11 50 44.6	11.20	1.08	1054	6489		Y	-GG	K0III-IV	RG,vis
814-1493	08 51 17.10	11 48 16.1	10.30	1.26	1016	6486		Y	-GG	K2III	RG
814-1685	08 51 17.36	11 47 00.7	13.06	0.57	998	5610		Y	D--		
814-2439	08 51 17.37	11 46 03.3	13.93	0.57	987	5608		Y	D--	G0V	
814-2331	08 51 17.48	11 45 22.7	9.72	1.37	978	6482		Y	-GG	K4III	RG
814-1827	08 51 18.01	11 45 54.3	12.73	0.55	986	5624	HV Cnc	Y	D--		EB
814-1803	08 51 18.70	11 47 02.9	12.60	0.78	999	5643	HW Cnc	Y	D--		
814-1937	08 51 19.93	11 47 00.5	12.13	0.46	997	5667		Y	D--	F1	BS
814-2405	08 51 20.10	12 18 10.4	9.37	1.48	1135	6495	BD+12 1924	?	-G-	K2	
814-1997	08 51 20.14	11 46 41.9	12.76	0.56	995	5675	NSV18058	Y	D--		
814-0963	08 51 20.17	11 52 48.2	13.84	0.60	1075	5692		Y	D--		
814-1975	08 51 20.35	11 45 52.6	13.15	0.57	2205	5679		Y	D--		
814-1811	08 51 20.56	11 46 05.0	13.18	0.57	988	5687		Y	D--		
814-2137	08 51 20.60	11 46 16.6	12.89	0.45	2204	5688	NSV18059	Y	D--	G:	BS
814-0889	08 51 20.79	11 53 26.2	11.25	0.42	1082	6493	ES Cnc	Y	DDD	F4	BS,EB
814-1975	08 51 21.24	11 45 52.8	12.26	0.57	984	5699		Y	D--	F5	BS
814-2231	08 51 21.56	11 46 06.0	11.44	1.06	989			Y	DGG		RG
814-1109	08 51 21.76	11 52 37.8	11.32	0.61	1072	6491		Y	DGG	G3III-IV	BS
814-0793	08 51 21.96	11 53 09.1	15.27	0.82	1079	5725		Y	D--	G8V	
814-1863	08 51 22.07	11 46 41.1	13.18	0.58	994	5716		Y	D--		
814-1531	08 51 22.81	11 48 01.7	10.48	1.11	1010	6485		Y	-GG	K2III	RG
814-1025	08 51 26.18	11 53 51.8	10.48	1.10	1084	6494		Y	-GG	G8III	RG
814-1911	08 51 26.44	11 43 50.6	11.28	0.13	968	6479		Y	DGG	A4.5:m	BS
814-1205	08 51 27.02	11 51 52.5	10.99	0.11	1066	6490		Y	-GG	A2V	BS
814-0601	08 51 27.44	12 07 40.7	8.28	0.32			HD 75638	N	-G-	F0	EB,vis
814-2319	08 51 28.15	11 49 27.4	12.78	0.49	1036	5833	EV Cnc	Y	-DD	F3	BS,EB
814-1147	08 51 28.98	11 50 33.0	10.55	1.12	1279	6503		Y	-GG	K1III	RG
814-1515	08 51 29.90	11 47 16.6	9.69	1.36	1250	6499	BD+12 1926	Y	-GG	K3III	RG
814-2079	08 51 30.50	11 48 57.0	12.11	1.01	1264	5877		N	-GG	F8	RG
814-1003	08 51 32.59	11 50 40.3	12.26	0.26	1280	5940	EW Cnc	Y	DDD	F0I	DS
814-2087	08 51 32.76	11 48 51.8	11.06	0.19	1263	6501		Y	-DD	A7III	BS
814-1315	08 51 34.32	11 51 10.4	10.94	0.22	1284	6504	EX Cnc	Y	-DD	A7	BS,DS
814-0741	08 51 35.79	11 53 34.7	12.23	0.99	1305	5997		Y	-GG	K0IV	RG
814-0847	08 51 37.20	11 59 02.4	11.10	0.85	1327	6507		N	-G-	G8	
814-1849	08 51 37.43	11 50 05.4	12.56	0.59	1275	6018		Y	D--	F9IV	
814-2291	08 51 37.85	11 50 57.0	13.33	0.56	1282	6027	AH Cnc	Y	-DD	F6.5	EB
814-1981	08 51 39.26	11 50 04.0	12.22	0.57	1273	6047		Y	D--	F8V	BS
814-1225	08 51 39.38	11 51 45.5	12.09	1.01	1293	6050		Y	-GG		RG
814-1007	08 51 42.34	11 50 07.5	11.63	1.05	1277	6502		Y	-GG		RG
814-1471	08 51 42.37	11 51 23.0	11.33	1.07	1288	6505		Y	-GG	K0	RG
814-1823	08 51 43.53	11 44 26.1	10.76	1.13	1221	6497		Y	-GG	K1III	RG
814-1619	08 51 43.87	11 56 42.2	10.58	1.10	1316	6506		Y	-GG	G8	
814-1591	08 51 45.08	11 47 45.9	11.52	1.05	1254	6500		Y	-GG	K0III	RG
814-2047	08 51 48.64	11 49 15.5	10.87	0.26	1267			?	DGG	A7V	
814-1171	08 51 49.12	11 49 43.8	12.73	0.58	1270	6166		Y	D--		
814-0795	08 51 49.35	11 53 39.0	7.98	1.11	1306	6193	HD75700	N	-GG	K0	
814-1463	08 51 49.97	11 49 31.4	12.65	0.58	1268	6177		Y	D--	F8	
814-1667	08 51 50.18	11 46 06.8	10.78	0.94	1237	6498		Y	-GG	G8III	RG
814-1011	08 51 56.01	11 51 25.9	10.60	0.34	1466	6511		Y	-GG	A3	BS
814-0817	08 51 59.51	11 55 04.5	10.55	1.10	1479	6512		Y	-GG	K1	RG
817-1563	08 52 01.93	13 23 26.3	8.96	0.23			HD75717	N	G--	F2	
814-0133	08 52 02.62	12 25 54.1	10.02	1.23	1533	6513	BD+12 1928	?	-G-	K0	
814-0323	08 52 10.65	12 17 51.9	9.89	0.47	1522		BD+12 1929	?	-G-		EB,vis

Table 1. (continued)

GSC	α	δ	V	$B - V$	Sand.	MMJ	Other	M67	Obs	Sp. type	Type
814-1881	08 52 10.72	11 44 05.1	10.70	0.11	1434	6510	BD+12 1930	?	-GG	A3III	
814-2361	08 52 18.56	11 44 26.2	10.47	1.12	1592	6516		Y	-GG	K0III	RG
817-1748	08 52 23.94	13 14 00.4	9.15	1.00			HD75784	N	G--	G5	
817-1469	08 52 24.12	13 16 06.2	9.86	0.39			BD+13 2006	N	G--		

Explanation of columns: GSC – Guide Star Catalog number; α, δ – ICRS equatorial coordinates for epoch and equinox 2000; $V, B - V$ – visual magnitude and colour index from Montgomery et al. (1993); Sand. – identification in Sanders (1977); MMJ – identification of star in Montgomery et al. (1993); Other – other designation; M67 – cluster membership according to Balaguer-Nunez et al. (2007); Obs – type of MOST observations in 2004, 2007 part A, 2007 part B: “D” Direct Imaging mode, “G” Guide Star mode, “-” not observed, (ES Cnc was observed both in Direct Imaging and Guide Star modes in 2007); Sp. type – spectral type; Type – general type and classification of the system: BS – blue straggler (Balaguer-Nunez et al. 2007), RG – red giant (Stello et al. 2007), EB – eclipsing binary, vis – visual pair, DS – δ Scuti variable.

Table 2. Parameters of the eclipsing systems AH Cnc, ES Cnc, and EV Cnc

	AH Cnc	ES Cnc		EV Cnc
Year	2007	2004	2007	2007
T_0	52790.9042(3)	52254.7811(11)		53245.087(4)
Period	0.36045713(21)	1.0677968(4)		0.4414399(17)
ΔV_p	0.33	0.114	0.121	0.148
ΔV_s	0.31	0.064	0.079	0.063
$\text{Max}_1 - \text{Max}_2$	0.00	0.016	0.027	-0.023

Explanation of columns: T_0 , Period – the linear ephemeris determined from our data as well as all published minima times, ΔV_p and ΔV_s – amplitudes of the primary and secondary minima, $\text{Max}_1 - \text{Max}_2$ – the O’Connell effect (positive if maximum following the primary minimum is fainter of the two).

the detailed discussion of spectroscopic observations and results see Pribulla et al., 2008, to be submitted to MNRAS).

3 LIGHT CURVES

For the known short-period eclipsing systems (AH Cnc, ES Cnc and EV Cnc) we constructed the phased light curves shown in Fig. 3. The data were first phased using linear ephemerides, determined using both published and new times of minimum light from the MOST photometry. Then the data were 3- σ -clipped to remove obvious outliers resulting mostly from cosmic ray hits. The number of outliers is strongly correlated with passages of the satellite through the SAA (South Atlantic Anomaly). Our final adopted parameters for AH Cnc, ES Cnc and EV Cnc are listed in Table 2.

In addition to the short-period binaries, we observed the long-period eclipsing binary HV Cnc and discovered two new eclipsing systems of this type, GSC 814-323 and HD75638. Light curves for phases close to eclipses for these three systems are plotted in Fig. 4. Our new minima for the systems, determined using the Kwee & van Woerden (1956) method, are listed in Table 3.

MOST photometry includes two known δ Scuti variables, EX Cnc and EW Cnc, and several blue stragglers which could possibly show period or quasi-periodic variations. The pulsations of EX Cnc are obvious and show beats of the two close periods (Fig. 5). We discuss photometry of the δ Scuti variables in Section 5.

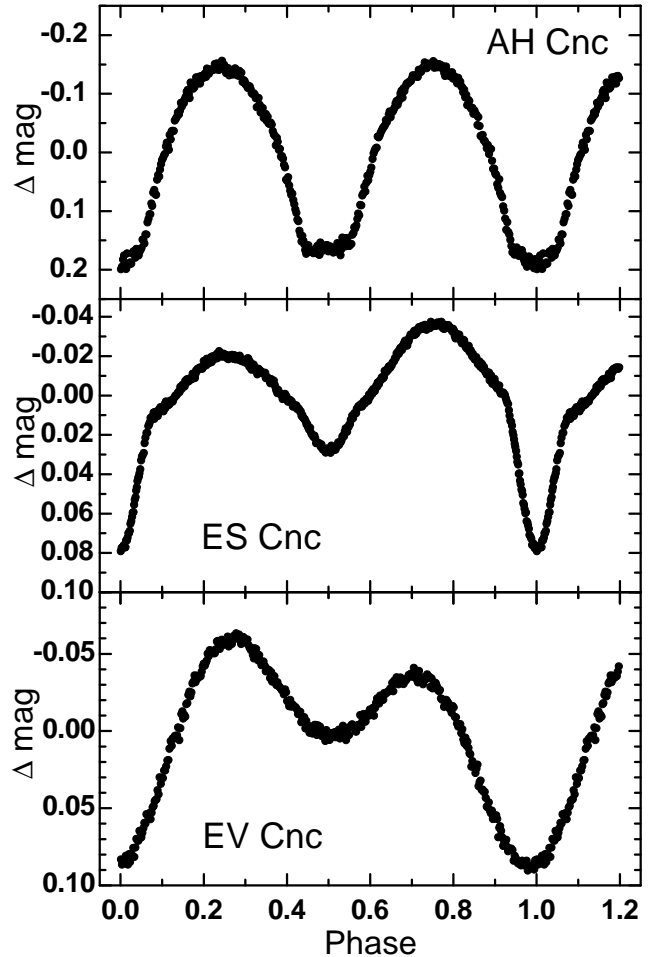


Figure 3. The phased light curves of three short-period eclipsing variable stars. AH Cnc and EV Cnc are contact binaries; ES Cnc is most probably a triple system containing an eclipsing contact binary. The light curves shown here are based on average data points computed from the entire MOST 2007 observing run. Note the very different vertical scales used in each of the panels.

4 ECLIPSING SYSTEMS AND BLUE STRAGGLERS

4.1 AH Cnc

AH Cnc (S1282, MMJ 6027) is a contact binary which is a member of the M67 cluster. The variability of this

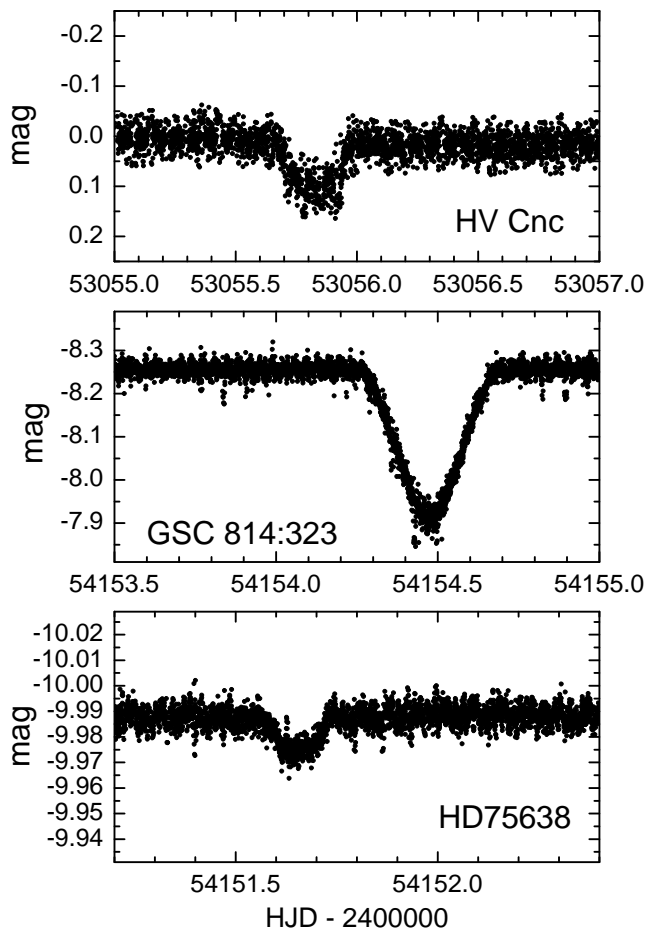


Figure 4. The light curves of the long-period eclipsing variables in the MOST M67 data. GSC 814–323 and HD 75638 are systems discovered during the MOST 2007 observing run while HV Cnc is an already known eclipsing system.

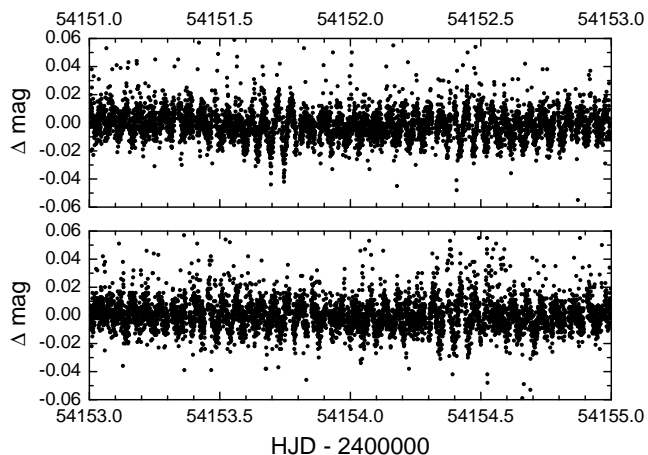


Figure 5. A four-day segment of the 2007 light curves of the δ Scuti variable EX Cnc. The wavelike variations correspond to a superposition of several close periodicities.

rather faint system ($V_{max} = 13.31$) was detected by Kurochkin (1960). Later the system was thoroughly studied by Whelan et al. (1979), who obtained both spectroscopic and photometric observations. The authors estimated its spectral type as F7V. The radial velocity orbit was, however, of limited quality. The geometric parameters were estimated as $i \sim 65 - 68^\circ$, $K_1 \sim 100 \text{ km s}^{-1}$, with a very uncertain mass ratio $q \sim 0.42 - 0.75$. An inspection of their light curves, with amplitude of about 0.38 mag, suggested partial eclipses and therefore a relatively high mass ratio.

Light curves of higher precision obtained by Gilliland et al. (1991) gave a very different picture: The system definitely showed total eclipses. The shallower of the two was flat, hence AH Cnc must be an A-type contact binary with the more massive component being hotter. Sandquist & Shetrone (2003a) presented a photometric analysis of their light curve indicating that the mass ratio can be as low as 0.16. More recent light curves from Zhang et al. (2005a) support a low mass ratio and clearly show an asymmetry which was interpreted as the presence of a dark photospheric spot. Finally, Qian et al. (2006) reported photometric evidence of a faint third component, contributing at most only about $L_3/(L_1 + L_2 + L_3) \approx 0.01$ and causing a cyclic ($P = 36.5 \text{ yr}$) variation in the observed times of minima.

Our phased light curve of AH Cnc is plotted in Fig. 3. The secondary minimum is flat and the light curve does not show any evidence of asymmetries. We fitted the light curve with the contact geometry Roche model, with the bolometric albedo and gravity darkening coefficients appropriate for the convective envelope. The effective temperature of the primary was set at $T_1 = 6220 \text{ K}$, corresponding to the F7V spectral type (and supported by its colour, see Table 1). Due to the strong correlation between the third light and mass ratio in the solution, for simplicity, we adopted zero third light. The resulting photometric elements, given in Table 4, confirm the low mass ratio, with the orbit oriented to us practically edge-on. Checks on the consistency of the solution can be made using the absolute magnitude calibration of Rucinski & Duerbeck (1997). Using the measured orbital period (Table 2) and de-reddened colour $(B - V)_0 = 0.51$, we obtain $M_V = 3.78$ with $V_{max} = 13.15$ (assuming $A_V = 3.2E_{B-V}$). This gives the distance modulus of $(m - M_V) = 9.37 \pm 0.02^2$, close to the value found for M67 by Nissen et al. (1987): $(m - M_V) = 9.61 \pm 0.04$. This consistent solution argues strongly against any third light in the system; such a third light would mean a lower brightness of the contact binary itself and a higher distance modulus, placing the star behind the cluster.

4.2 ES Cnc

ES Cnc (S1082, MMJ 6493, spectral type F4) is a very complex, probably best studied blue-straggler eclipsing system in M67. Its photometric variability was discovered by Simoda (1991). Later, Goranskij et al. (1992) discovered that it is a close binary showing partial eclipses with an orbital period of 1.0677978(50) d. However, Milone & Latham

² uncertainty is here mainly given by intrinsic differences between the individual binary systems and can be estimated as $\pm 0.2 \text{ mag}$

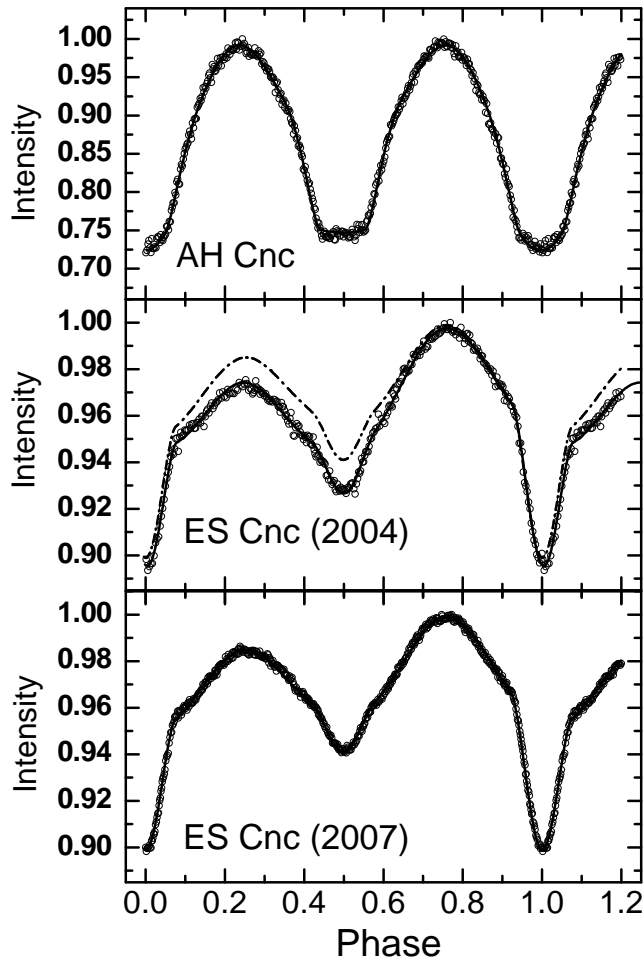


Figure 6. The best fits to the light curves of AH Cnc (top) and both MOST 2004 and 2007 light curves of ES Cnc obtained assuming the contact model. In the case of ES Cnc, two cool spots on the primary component are necessary to explain the observed asymmetry. The panel with the 2004 light curve contains for comparison the shape of the 2007 light curve (dot-dashed line).

(1992) found some radial velocity variability, but no sign of the 1.07 d period.

A real breakthrough in the understanding of ES Cnc system was made by van den Berg et al. (2001), who found that in addition to the slowly moving, narrow-line component (later found to be moving in a 1189-d orbit (Sandquist et al. 2003)), the spectrum of the system contains two other components. Their radial velocities vary with the orbital period of 1.07 d, so the system is a hierarchical triple in which all three components are blue stragglers. Both van den Berg et al. (2001) and Goranskij et al. (1992) noted that the maximum following the primary minimum is brighter by 0.01 – 0.02 mag. This, together with strong X-ray flux (Belloni et al. 1998) indicates that the close pair is a magnetically active, RS CVn-like eclipsing binary. Further extensive photometric observations by Sandquist et al. (2003) showed that the light curve of the system is variable at a level of about 0.02 mag and on a timescale of about a month. The authors noted a short timescale variation of the brightness, which they interpreted as δ Sct-type variability of the third component.

Table 3. New primary minima of eclipsing systems determined from the MOST observations. The epochs for ES Cnc and EV Cnc correspond to ephemerides given in Table 2. The epoch for the minimum of HV Cnc is counted from T_0 in the ephemeris of Sandquist & Shetrone (2003b).

Epoch	HJD 2 400 000+	Epoch	HJD 2 400 000+
ES Cnc		8918	54165.8639
7874	53051.0877	8920	54167.9957
7876	53053.2117	8922	54170.1339
7877	53054.2879	8923	54171.2019
7878	53055.3548	8924	54172.2696
7879	53056.4249	8925	54173.3370
7880	53057.4922	EV Cnc	
7881	53058.5610	8255	54144.1280
8898	54144.5101	8262	54147.2024
8899	54145.5763	8263	54147.6584
8901	54147.7092	8269	54150.3054
8902	54148.7871	8272	54151.6301
8903	54149.8446	8273	54152.0721
8904	54150.9149	8274	54152.5075
8905	54151.9802	HV Cnc	
8906	54153.0473	703	53055.828
8907	54154.1151	GSC 814-323	
8908	54155.1824	0	54154.481
8910	54157.3186	HD 75638	
8912	54159.4546	0	54145.85
8913	54160.5220	1	54151.65
8914	54161.5918	2	54157.47

The system was comfortably bright for MOST photometry, with a typical standard error per individual measurement of $\sigma \sim 0.006 - 0.01$ mag. However, there exist some very long-term trends in the MOST 2004 and 2007 data, probably associated with evolution of scattered Earthshine in the field during the runs, so we conservatively choose not to use MOST photometry to interpret any slow variability in ES Cnc. Instead, we constructed the phased, seasonal light curves (Fig. 3) from σ -clipped data, to enhance the precision of our photometry to the level of the point-to-point error of only 1.1 mmag for the 2007 data. Our light curves show the O’Connell effect during both seasons, in 2004 and in 2007, in contrast to what was reported by van den Berg et al. (2001) and Goranskij et al. (1992). In spite of the continuous variations due to the spots and the ellipticity effect, the outer contacts of the eclipses are exceptionally well defined, especially in the 2007 light curve.

The light curve of ES Cnc was modelled first for the 2007 data. We assumed a spectroscopic mass ratio of $q_{sp} = 0.63$ (Sandquist et al. 2003) and effective temperature of the primary $T_{eff} = 7325$ K (the primary temperature from Table 5 of Sandquist et al. (2003)). Both the bolometric albedo and the gravity darkening coefficients were set following van den Berg et al. (2001). The asymmetry of the light curve, which is very probably caused by photospheric spots, is significant but very stable, so we assume – unlike van den Berg et al. (2001) – synchronous rotation of the components. The third light was optimised in the solution. Immediately after a few trial runs, we realized that the deformation of the observed light curve cannot be explained by one dark spot, and that at least two spots are necessary. Experimentation with the temperature factor k of the spot (the ratio of the spot temperature and photospheric temperature outside the spot; Linnell (1993)) showed that spots are rather cool with $k \sim 0.85$ and are small in size.

Our solution (Fig. 6 and Table 4) fits the observed light curve well. Because of the ill posed nature of this type of fitting, the solution is not unique: A fit of a similar quality can be obtained by placing the spots at different latitudes, because the spot diameter correlates strongly with the temperature factor. Also, since the spots are not eclipsed, it is hard to determine from the photometry alone which of the components is spotted.

The 2004 light curve was fitted with the same assumptions as for the 2007 light curve, i.e., the geometric elements were fixed by the solution of the 2007 light curve. The 2004 phased light curve shows a larger asymmetry than in 2007, but of the same sense: The maximum following the primary minimum is fainter. The resulting fit is shown in Fig. 6. As expected, the spot radii are larger than in the 2007 fit. The spots, however, seem to have hardly moved between 2004 and 2007.

In spite of the very good reproduction of the observations by our model, we still regard the resulting parameters (Table 4) as preliminary because of the large asymmetry and our inability to determine parameters free of spot effects (see Sandquist et al. (2003)). Some systematic uncertainty might arise from the very broad transmission of the MOST broadband filter and slightly variable colours during the orbital revolution. The ES Cnc system calls for thorough modelling of simultaneously observed line profiles (or BFs) and photometric data.

The $O - C$ diagram for all available minima of ES Cnc shows a rather high scatter. An attempt to interpret the deviations as due to the light-time effect (hereafter LITE) caused by the third component led to a substantially longer orbital period ($P1304 \pm 13$ days) than indicated by spectroscopy, $P = 1188.5 \pm 6.76$ days (Sandquist et al. 2003). The problem is very probably caused by (i) the low amplitude of LITE due to the short orbital period, (ii) the shallow eclipses making their positions rather poorly determined, and (iii) a large and variable O’Connell effect causing the apparent instants of minima to deviate from the spectroscopic conjunctions as defined by the component’s centres of mass. Without more highly precise and reliable timings of the minima, any conclusions about the possible LITE orbit are a premature speculation. On the other hand, the presence of LITE would conclusively settle the physical bond of the triple system as the third body may be simply an optical projection within the cluster.

4.3 EV Cnc

EV Cnc (S1036, MMJ 5833, spectral type F3) is another blue straggler binary. The system is very probably close to contact or perhaps already in contact, and is seen at low inclination. The light curve of the system is rather unusual: Although the light curve is continuous, indicating the contact binary nature of the system, the depths of minima are significantly different, hardly consistent with the components being in contact. Also, the maximum following the primary minimum is about 0.025 mag brighter than the other maximum. The system was initially detected by Gilliland et al. (1991) and extensively studied by Sandquist & Shetrone (2003a), who improved the ephemeris for minimum light to $T_0 = 2450500.047 + 0.441437(3) \times E$. Their grid-search approach to find the most probable geometric and spot pa-

Table 4. Photometric light curve solutions for the short-period eclipsing systems

Parameter	AH Cnc (2007)	ES Cnc (2004)	ES Cnc (2007)
i [deg]	89.5	66.2	66.2
Ω_1	2.023	3.532 ^f	3.532
Ω_2	2.023	3.922 ^f	3.922
q	0.130	0.63 ^f	0.63 ^f
T_1 [K]	6300	7325 ^f	7325 ^f
T_2 [K]	6368	5543	5543
l_3	0.00 ^f	0.68	0.68
A_1	0.50 ^f	1.00 ^f	1.00 ^f
A_2	0.50 ^f	0.50 ^f	0.50 ^f
g_1	0.25 ^f	1.00 ^f	1.00 ^f
g_2	0.25 ^f	0.25 ^f	0.25 ^f
k^s	–	0.80 ^f	0.80 ^f
r_{I1}^s [deg]	–	15.35	11.5
l_{I1}^s [deg]	–	187.2	179.9
r_{II1}^s [deg]	–	15.75	12.5
l_{II1}^s [deg]	–	293.9	296.6

Explanation of rows: i – inclination angle; Ω – dimensionless surface potential; $q = m_2/m_1$ – mass ratio; $T_{1,2}$ – polar temperature; $l_3 = L_3/(L_1 + L_2 + L_3)$ – third light; $A_{1,2}$ – bolometric albedo; $g_{1,2}$ – gravity darkening coefficient; k^s – temperature factor of spot(s), and $r_{1,2}^s$ and $l_{1,2}^s$ – longitude and radius of the first and the second spot. Indices 1, 2, 3 denote components while I, II identify the spots.

rameters led to a fairly uncertain result, exacerbated by the lack of a spectroscopic mass ratio, q_{sp} . If the system is in contact, its inclination angle is $30^\circ < i < 38^\circ$, its mass ratio is $q_{ph} \sim 0.5$ and at least two dark spots are required to reproduce the light curve. Sandquist & Shetrone (2003a) noted small variations in the shape of the phase diagram on timescales of about a month.

Our MOST photometry allowed us to determine reliably 10 new times of minimum for EV Cnc (Table 3). Combining our new minima with the published ones leads to an improvement of the ephemeris to $T_0 = 2453245.087(4) + 0.4414399(17) \times E$. Our light curve (Fig. 3), shows a very similar shape to that of Sandquist & Shetrone (2003a) or Gilliland et al. (1991), indicating very stable surface structures, similar to the behaviour found in the contact binary AG Vir (Bell et al. 1990). We attempted to model the light curve of EV Cnc but we found that there are many combinations of parameters leading to similar quality fits. Thus, we could add little to the discussion of Sandquist & Shetrone (2003a). Furthermore, we found that the temperature of the secondary component T_2 cannot be determined reliably because of the strong correlation between T_2 , the fill-out factor, and the inclination angle. Any further progress in understanding EV Cnc requires a dedicated spectroscopic study providing a reliable mass ratio.

4.4 HV Cnc

HV Cnc (S986, MMJ 5624) is very probably a member of M67 (Balaguer-Nunez et al. 2007). Spectroscopic observations by Mathieu et al. (1990) show that the system is a single-lined spectroscopic binary (SB1) with a circular orbit and a period of 10.3386 days. Eclipses were observed later by Sandquist & Shetrone (2003b). The authors found another component in the spectra which they identified with

a third star in the system, contributing about 11.5% to the total light. Through a deconvolution of the photometry of all three stars, it was found that the primary is hotter than the turn-off point of the cluster so it is a Blue Straggler.

HV Cnc was observed by the MOST satellite only during the 2004 observing run. One primary minimum at HJD 2453 055.828 was observed. The minimum occurred very close to the time predicted by the ephemeris of Sandquist & Shetrone (2003b), at phase 0.99928, proving that the orbital period is very stable. No mass transfer or stronger interactions of components is possible for such a relatively long orbital period. HV Cnc is rather faint for MOST photometry ($V_{max} = 12.73$), especially early in the mission, and the data show a scatter as large as 0.02 mag, so that secondary minima could not be detected. No spectra of HV Cnc were obtained at DDO because the system is too faint for the 1.88m telescope.

4.5 GSC 814-323

GSC 814-323 (S1522, BD +12°1929) is most probably not a member of M67 (Zhao et al. 1993). It is, however, a visual pair (WDS 08522+1217) consisting of stars with $V = 9.12$ and $V = 10.21$ separated by $\rho = 14.4$ arcsec at a position angle $\theta = 140^\circ$.

The MOST photometry revealed a single, well-defined, partial eclipse centred at HJD 2454 154.481 and lasting about 9 hours. The brightness of the system dropped by 0.33 mag (Fig 4). Since the system was observed in the guide star mode (processed on board the satellite) and the MOST focal plane scale is 3 arcsec/pixel, the photometry is expected to include both visual components. If the brighter component is the eclipsing binary, then the corrected amplitude of the eclipse would be about 0.48 mag. The fainter component cannot be responsible for the eclipse because even its total exclusion would result in a drop of 0.34 mag in brightness.

Unfortunately, only one eclipse was recorded during the first part of the MOST 2007 run, setting a lower limit on the orbital period of about 11 days. The system was not detected as a variable during the ASAS³ nor the NSVS⁴ variability surveys.

There is a single radial velocity measurement of GSC 814-323 at HJD 2441 321.88 published by Mathieu et al. (1986), giving $RV = 12.6(5)$ km s⁻¹. The measurement probably refers to the brighter component of the visual pair. Two spectra taken at DDO suggest that the system is a double-lined spectroscopic binary (SB2); see Fig. 2. The ratio of intensities, as estimated from the BFs when the components are split, is about $L_2/L_1 \sim 0.29$. Therefore, we could expect secondary eclipses about 0.09 mag deep. More spectra are needed to find the orbital period and to characterise this triple system.

4.6 HD 75638

HD75638 (GSC 814-601, BD +12°1925; spectral type F0) is another field star close to M67. The star is, in fact, a known visual triple system (WDS 08515+1208) consisting

of components A ($V = 8.28$), B ($V = 10.17$) and C ($V = 11.8$). While the pair AB is rather tight ($\rho = 1.4$ arcsec), the faintest component C is separated by 15.1 arcsec from the brightest one; it is too far to contribute to the aperture photometry used for the MOST data.

HD 75638 (components AB) was found to be an SB3 system in the survey of Nordstroem et al. (1997). Analysis of 13 spectra showed two measurable components with $v_1 \sin i = 80$ km s⁻¹ and $v_2 \sin i = 10$ km s⁻¹, temperatures $T_1 = 7000K$, and $T_2 = 6750K$, and a luminosity ratio of 0.10. A preliminary orbit for the fainter component was given: $P = 5.8167(9)$ days, $V_0 = 11.05(91)$ km s⁻¹, $K_1 = 28.9(12)$ km s⁻¹, $e = 0.083(56)$, and $\omega = 322(28)^\circ$. The spectroscopic orbit most likely corresponds to the motion of the blend of a faint pair seen as component B.

The system was used as a guide star in the MOST 2007 observations of M67. The photometry covers three consecutive eclipses. The eclipse depth is very shallow (only about 0.013 mag) and the eclipses are total (see Fig. 4). It is very probable that it is the fainter component of the close visual pair (component B) which is the eclipsing binary with its light being diluted by the brighter component. In such a case, the original, undiluted amplitude of eclipses would be 0.09 mag. Since the eclipses are total, the ratio of radii can be determined to be $R_2/R_1 = 0.3$. The preliminary mid-eclipse ephemeris is HJD 2454 145.85 + 5.81 × E days.

Our spectroscopy included the AB pair, which could not be separated at the spectrograph slit because the typical seeing at the site (~ 2 arcsec) is larger than the separation of the pair. The broadening functions (Fig. 2) show the brighter, rapidly-rotating component ($v \sin i \approx 85$ km s⁻¹) to be stationary in radial velocity; this star is most likely the A component of the visual pair. The fainter component shows radial velocity variations and is definitely responsible for the eclipses. Our three spectra show that the features of the eclipsing pair are always blended, suggesting that high-resolution spectroscopy will be necessary to reliably define orbits of both components.

5 δ SCUTI PULSATING STARS IN M67

The quality of the MOST data varied over the two runs and depended on the position of the target on the CCD chip mainly because of time and spatial dependence of the stray light and/or background. For faint pulsating stars observed in the M67 field, the instrumentally introduced periodicities affected the period analysis and its conclusions and limited our ability to detect very small amplitude pulsations. The direct imaging objects could in general be followed through the whole satellite orbit so that the data were entirely suitable for the period analysis but for the guide stars, the background variation led to exclusion of about 20% of the satellite period. For both sets of data, however, intermittent gaps occurred hence we used the method of Deeming (1975) of period finding with Fourier transform of unevenly spaced data points. It turned out that all stars observed in the guide star mode were unsuitable for a sound periodic analysis. Thus, we cannot say anything about any of the remaining observed blue stragglers, Sanders 752, 968, 977, 1066, and 1466, which show the frequency spectrum dominated by the satellite orbital frequency 14.1994 c/day and its integer multiples. The

³ (<http://archive.princeton.edu/~asas/>)

⁴ (<http://skydot.lanl.gov/nsvs/nsvs.php>)

second strong periodicity in the data (1 c/day) arises from the periodic returns of the satellite to the Earthshine illumination conditions, which determine the background level. Thus, for these stars, any intrinsic variability must have amplitudes smaller than about 0.001 mag; this limit also applies to Sanders 1263 which was observed in the raster mode.

Because the direct imaging observations were almost continuous, the spectral window for such observations is virtually free of aliasing. The spectral window for the guide stars shows strong side-lobes corresponding the orbital frequency of the satellite.

5.1 EX Cnc

EX Cnc (S1284, MMJ 6504) is very probably member of M67 (Balaguer-Nunez et al. 2007). Its variability was discovered by Gilliland et al. (1991) and later studied by Gilliland & Brown (1992) and Zhang et al. (2005b). The most detailed investigation of this δ Sct variable resulted from the large multi-site campaign of Bruntt et al. (2007). The authors presented photometric data from eight sites using nine telescopes of 0.6 m to 2.1 m, performed over 43 days. The authors were able to detect 26 frequencies in their data, but the spectral window was poor and contained rather strong side-lobes.

EX Cnc was observed by the MOST satellite almost continuously over 30 days in 2007. The pulsations and their beating are directly visible in the data (see Fig. 5). After the change of the satellite roll angle during the 2007 run, the data were of lower quality. For that reason, only the best and the least interrupted continuous part of the run was selected for the period analysis within $HJD2454149.7 - 2454163.1$. Although the per-point error is about 0.01 mag, the run is homogeneous and the spectral window is practically single peaked; the only side-lobes with less than 10% strength correspond to the satellite orbital cycle at the frequencies ± 14.2 c/day. The amplitude spectrum and the corresponding spectral window are shown in Fig. 7.

The total number of reliably detected frequencies for EX Cnc is over 20 with most corresponding to 26 frequencies detected by Bruntt et al. (2007). The accord between the results is surprisingly good: out of the 22 strongest frequencies detected by Bruntt et al. (2007) we could find 20. Because our useful observing window is shorter, we could not resolve several close pairs of frequencies resolved by the authors. Except for the frequencies found by the authors, we found few additional modes at 20.855 c/day, 29.385 c/day, 13.205 c/day and 15.19 c/d. The last two, however, could be connected with the orbital period of the satellite. EX Cnc was not observed during the 2004 run. All identified frequencies in the amplitude spectrum are listed in Table 5.

5.2 EW Cnc

EW Cnc (S1280, MMJ 5904) is very probably a member of M67 (Balaguer-Nunez et al. 2007). The system has a very similar history to EX Cnc since its discovery by Gilliland et al. (1991), who found that it is a δ Sct variable. Bruntt et al. (2007) claimed to detect as many as 41 frequencies in their photometry. Unfortunately, EW Cnc was a rather faint target for the MOST satellite which resulted in

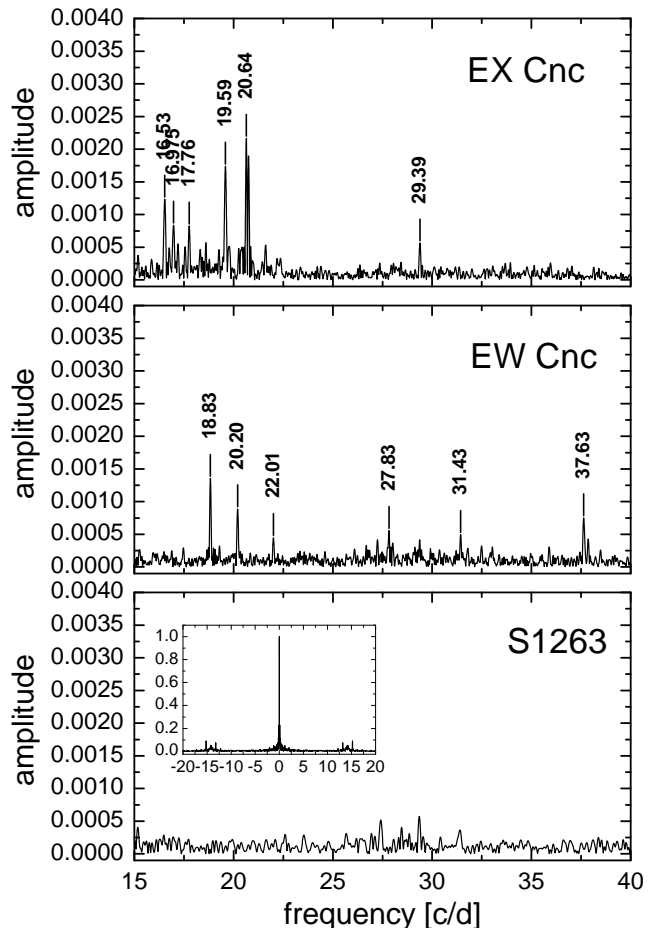


Figure 7. The amplitude spectra obtained from the 2007 observations for three blue stragglers observed in the raster mode, EX Cnc, EW Cnc, and S1263. While the first two objects clearly show the presence of δ Sct-type pulsations, S1263 does not show any detectable variability in the analyzed frequency range (2 – 200 c/day). The spectral window given in the S1263 panel is approximately valid for all three stars.

a 0.02 mag point-to-point scatter in the (generally better of the two runs) 2007 data. The scatter of data substantially varied, hence we selected the best and most continuous segment for the period analysis (between $HJD2454145.22 - 2464160$). The brightness variations caused by the δ Sct-type pulsations are barely detectable by visual inspection of the light curve. Nevertheless, eight frequencies are clearly visible in the 2007 amplitude spectrum; the strongest six practically coincide with those detected in the more precise data of both Gilliland & Brown (1992) and Bruntt et al. (2007). EW Cnc was also observed during the shorter observing run in 2004. The amplitude spectrum shows three frequencies: 18.83, 27.85 and 20.20 c/day; the same as detected from the 2007 run data (see Fig. 7, Table 5) and found by Bruntt et al. (2007). This indicates that the pulsation modes are highly stable over long time intervals.

6 CONCLUSIONS

Two long, almost continuous photometric runs (10 days in 2004 and 30 days in 2007) of stars in the M67 field were

Table 5. Pulsation frequencies and their amplitudes detected in the 2007 MOST photometry. Frequencies are given both in cycles per day and μHz ; amplitudes are given in millimagnitudes. Identifications of particular frequencies in Bruntt et al. (2007) are given in the last column

No.	frequency [c/day]	frequency [μHz]	Amplitude [mmag]	Identification
EX Cnc				
1	20.640	238.89	2.17	f_2
2	20.753	240.20	1.90	f_1
3	19.589	226.72	1.74	$f_{3,5}$
4	16.531	191.33	1.23	$f_{4,10}$
5	16.974	196.46	0.84	$f_{9,13}$
6	17.761	205.57	0.82	f_6
7	18.603	215.31	0.57	f_8
8	29.385	340.10	0.56	
9	17.198	199.05	0.55	$f_{20}?$
10	21.613	250.15	0.53	$f_{23}?$
11	20.856	241.39	0.51	
12	17.556	203.19	0.51	f_{17}
13	19.777	228.90	0.51	$f_{7,22}$
14	20.428	236.44	0.50	f_{16}
15	20.530	237.62	0.50	
16	16.758	193.96	0.49	f_{14}
17	20.260	234.50	0.48	f_{21}
18	18.321	212.05	0.46	f_{12}
19	19.262	222.94	0.46	f_{18}
20	13.21	152.9	0.41	
21	15.19	175.8	0.37	
22	18.42	213.2	0.35	
23	22.19	256.8	0.33	f_{24}
24	22.36	258.8	0.33	f_{19}
25	18.78	217.4	0.32	f_{11}
26	15.87	183.7	0.32	
EW Cnc				
1	18.834	217.99	1.35	f_1
2	20.198	233.77	0.89	f_2
3	37.632	435.56	0.75	f_5
4	27.828	322.08	0.56	f_4
5	31.432	363.80	0.50	f_3
6	22.008	254.72	0.49	f_6
7	37.86	438.2	0.43	
8	27.25	315.4	0.42	$f_{40}?$

obtained by the MOST space mission, followed by ground based spectroscopic observations at DDO. The targets include eclipsing blue stragglers in M67, δ Scuti-type pulsating star, and variable non-cluster members in the cluster field.

Among the main results, our analysis of the light curve of the contact binary AH Cnc supports its low mass ratio and a high inclination angle, as found by Sandquist & Shetrone (2003a). Contrary to a recent suggestion, there is no compelling evidence for a third component in the system. The MOST light curves of the blue straggler triple system ES Cnc show a clear asymmetry which we interpret as the presence of two dark photospheric spots, about 1200 K cooler than the surrounding photosphere. A comparison of the 2004 and 2007 photometry reveals almost no changes in the fitted sizes and positions of the spots, suggesting a surprising stability in the photospheric features of the components over three years. However, our analysis of ES Cnc is only preliminary. The system deserves a dedicated campaign of high-resolution spectroscopy and simultaneous high-precision photometry, but the proximity of its period to one day is a somewhat complicating factor.

Two new field eclipsing systems were discovered: HD 75638 and GSC 814-323. The former is a known spectroscopic triple. The eclipses are very shallow ($A \sim 0.013$ mag) and would be barely detectable from the ground. The

photometric period (the mean interval between the eclipses) of 5.81 days is compatible with the spectroscopic period of 5.8167 days found from observations spanning 3.68 years by Nordstroem et al. (1997). High-resolution spectroscopy of the system combined with our light curve could lead to reliable determination of masses of all three components. Spectra of GSC 814-323 show that it is a spectroscopic binary. Since the ratio of intensities of the components in the broadening functions is about 0.29, we expect the secondary eclipses to be 0.09 mag deep.

Period analysis of two known δ Scuti variables, EX Cnc and EW Cnc yielded a very reliable frequency spectrum without any obvious instrumental periodicities. For the brighter of the two variables, EX Cnc, we could reliably determine as many as 26 pulsational frequencies. In spite of the larger photometric scatter of about 0.02 mag for the fainter variable, EW Cnc, we see 8 pulsation frequencies in the amplitude spectrum. Pulsational frequencies in both stars are temporary highly stable. The guide star photometry of other blue stragglers (Sanders 752, 968, 977, 1066, and 1466) was affected by the strong background variations which limited amplitudes of any detectable pulsations to < 0.001 mag.

ACKNOWLEDGMENTS

This study has been funded by the Canadian Space Agency Space Enhancement Program (SSEP) with TP holding a Post-Doctoral Fellowship position at the University of Toronto. The Natural Sciences and Engineering Research Council of Canada (NSERC) supports the research of DBG, JMM, AFJM, and SMR. Additional support for AFJM comes from FQRNT (Quebec). RK is supported by the Canadian Space Agency and WWW is supported by the Austrian Space Agency and the Austrian Science Fund (P17580). This research has made use of the SIMBAD database, operated at CDS, Strasbourg, France and NASA's Astrophysics Data System Bibliographic Services.

REFERENCES

- Bailyn C.D. 1995, ARA&A, 33, 133
 Balaguer-Nunez L., Galadi-Enriquez D., Jordi C. 2007, A&A, 470, 585
 Bell S.A., Rainger P., Hilditch R.W. 1990, MNRAS, 247, 632
 Belloni T., Verbunt F., Mathieu R.D. 1998, A&A, 339, 431
 Bruntt H., Stello D., Suárez J.C., Arentoft T., Bedding T.R., Bouzid M.Y., Csubry Z., Dall T.H., Dind Z.E., Frandsen S., Gilliland R.L., Jacob A.P., Jensen H.R., Kang Y.B., Kim S.-L., Kiss L.L., Kjeldsen H., Koo J.-R., Lee J.-A., Lee C.-U., Nuspl J., Sterken C., Szabó R. 2007, MNRAS, 378, 1371
 Deeming T.J. 1975, Ap&SS, 36, 137
 European Space Agency 1997, The Hipparcos and Tycho Catalogues (ESA SP-1200)(Noordwijk: ESA) (HIP)
 Gilliland R.L., Brown T.M. 1992, AJ, 103, 1945
 Gilliland R.L., Brown T.M., Duncan D.K., Suntzeff N.B., Lockwood G.W., Thompson D., Schild R.E., Jeffrey W.A., Penprase B.E. 1991, AJ, 101, 541

- Goranskij V.P., Kusakin A.V., Mironov A.V., Moshkaljov V.G., Pastukhova E.N. 1992, *Astron. Astrophys. Trans.*, 2, 201
- Høg E., Fabricius C., Makarov V.V., Urban S., Corbin T., Wycoff G., Bastian U., Schwekendiek P., & Wicenec A. 2000, *A&A*, 355, 27L
- Kurochkin N.E. 1960, *Astron. Tsirk.*, 212, 9
- Kwee K.K., van Woerden H. 1956, *Bulletin of the Astronomical Institutes of the Netherlands*, 12, 327
- Latham D.W., Milone A.A.E. 1996, in *The Origins, Evolution, and Destinies of Binary Stars in Clusters*, ed. E. Milone & J.C. Mermilliod, *ASP Conf. Series*, 90, 385
- Linnell A.P. 1993, in *Light curve modeling of eclipsing binary stars*, ed. E.F. Milone, p103
- Mathieu R.D., Latham D.W., Griffin R.F., Gunn J.E. 1986, *AJ*, 92, 1100
- Mathieu R.D., Latham D.W., Griffin R.F. 1986, *AJ*, 100, 1859
- Matthews J.M., Kusching R., Guenther D.B., Walker G.A.H., Moffat A.F.J., Rucinski S.M., Sasselov D., Weiss W.W. 2004, *Nature*, 430, 51
- Milone A.A.E., Latham D.W. 1992, in *Evolutionary Processes in Interacting Binary Stars*, ed. Kondo Y. et al., 475
- Montgomery K.A., Marschall L.A., Janes K.A. 1993, *AJ*, 106, 181
- Nissen P.E., Twarog B.A. Crawford D.L. 1987, *AJ*, 93, 634
- Nordstrom B., Stefanik R.P., Latham D.W., Andersen J. 1997, *A&AS*, 126, 21
- Pribulla T. 2004, in *Spectroscopically and Spatially Resolving the Components of the Close Binary Stars*, ed. Hilditch R.W. et al., *ASP Conf. Series*, 318, 117
- Pribulla T., Rucinski S.M., Lu W., Mochnacki S.W., Conidis G., DeBond H., Thomson J.R., Pych W., Blake R.M., Ogloza W., Siwak M. 2006, *AJ*, 132, 769
- Pych W. 2004, *PASP*, 116, 148
- Qian S.B, Liu L., Soonthornthum B., Zhu L.Y., He J.J. 2006, *AJ*, 131, 3028
- Rucinski S.M., 1992, *AJ*, 104, 1968
- Rucinski S.M. 2002, *AJ*, 124, 1746
- Rucinski S.M., Duerbeck H.W. 1997, *PASP*, 109, 1340
- Sanders W.L., 1977, *A&AS*, 27, 89
- Sandquist E.L., Shetrone M.D. 2003, *AJ*, 125, 2173
- Sandquist E.L., Shetrone M.D. 2003, *AJ*, 126, 2954
- Sandquist E.L., Latham D.W., Shetrone M.D., Milone A.A.E. 2003, *AJ*, 125, 810
- Simoda M. 1991, *Inf. Bull. Variable Stars*, No. 3675
- Stello, D., Bruntt, H., Kjeldsen, H., Bedding, T.R., Arentoft, T. Gilliland, R.L., Nuspl, J., Kim, S.-L., Kang, Y.B., Koo, J.-R., Lee, J.-A., Sterken, C., Lee, C.U., Jensen, H.R., Jacob, A.P., Szabó, R., Frandsen, S., Csubry, Z., Dind, Z.E., Bouzid, M.Y., Dall, T.H., Kiss, L.L. 2007, *MNRAS* 377, 584
- Walker G., Matthews J., Kuschnig R., Johnson R., Rucinski S., Pazder J., Burley G., Walker A., Skaret K., Zee R., Grocott S., Carroll K., Sinclair P., Sturgeon D., Harron J. 2003, *PASP*, 115, 1023
- van den Berg M., Orosz J., Verbunt F., Stassun K. 2001, *A&A*, 375, 375
- van Hamme W. 1993, *AJ*, 106, 2096
- Whelan J.A.J., Worden S.P., Rucinski S.M., Romanishin W. 1979, *MNRAS*, 186, 729
- Zhang X.B., Zhang R.X., Deng L. 2005a, *AJ*, 129, 979
- Zhang X.B., Zhang R.X., Li, Z.P. 2005b, *Chin. J. Astron. Astrophys.*, 5, 579
- Zhao J.L., Tian K.P., Pan R.S., He Y.P., Shi H.M. 1993, *A&AS*, 100, 243